A Novel Modulation Strategy for Active Rectification of A Snubber Less Soft-switched Single Stage 3ϕ High Frequency Link DC-AC Converter

Anirban Pal and Kaushik Basu
Department of Electrical Engineering,
Indian Institute of Science, Bangalore- 560012, India
Email: palanirban@ee.iisc.ernet.in, basu@ee.iisc.ernet.in

***Abstract*—This paper proposes a novel modulation strategy for active rectification of a single stage, isolated, three-phase high frequency link DC-AC converter. The proposed modulation strategy results in zero voltage switching (ZVS) of the DC side converter and zero current switching (ZCS) of AC side converter at all operating conditions without using additional snubber circuit. The technique also ensures magnetic flux balance of transformer within a switching cycle. High frequency transformer (HFT) flux balance results in significant reduction in size and weight and hence improves power density. The paper presents a detailed description of the proposed modulation strategy for unity power factor (UPF) operation. Important simulation results are shown to verify the converter operation.**

Keywords- cycloconverter, modulation technique, high-frequency-AC-link, zero-voltage switching (ZVS), zero-current switching (ZCS)

I. Introduction

The single stage three-phase high frequency link DC-AC converter as shown in Fig. 1, is becoming popular for applications like grid integration of renewable sources, energy storage system, hybrid and electric vehicle, vehicle to grid (V2G) integration, uninterruptible power supplies (UPS) etc. It has some attractive features such as- direct conversion of high frequency AC to line frequency AC, bidirectional power transfer capability, high power density, lower weight etc. The topology has been widely discussed in literature [1]–[4]. Different techniques to achieve soft switching of the AC side cycloconverter are studied. In [1], a modulation strategy for DC to AC side power flow is discussed. In this paper a ZCS scheme is implemented for the DC side H-bridge but transformer leakage commutation is ignored. In [2], a source based leakage energy commutation technique is described and implemented for DC to AC power flow case that results ZCS in the AC side cycloconverter. Paper [3] describes a space vector based modulation technique for DC to AC power flow which results non resonant ZVS switching of the cycloconverter. In [4] DC to AC power flow is discussed and it uses an additional RC snubber to suppress voltage oscillation. A soft-switching technique is given in [5] for AC to DC side power flow but detailed modulation strategy is not discussed. In [6] a modulation strategy is presented for DC to AC side power flow with unity power factor (UPF) operation which results soft switching of the converter. In [6] following space vector sequence is applied over a switching cycle when the reference output voltage vector is in sector I_b (in Fig. 3) : (V_7-V_2-V_1)-(V_7-V_1). Due to asymmetry in switching sequence transformer flux has low frequency component (3 times the line frequency).

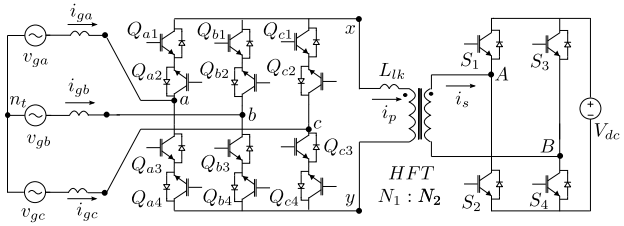

Fig. 1. Single-stage high-frequency link 3ϕ AC-DC converter

978-1-5386-1379-5/17/$31.00 © 2017 IEEE

In this paper a novel switching strategy is proposed for AC to DC power flow. The proposed scheme results in- 1) high frequency flux balance: transformer flux is balanced over a switching cycle, 2) snubber less soft switching at all load: ZCS in AC side Cyclo-converter and ZVS in DC side H-bridge, 3) active rectification at UPF. The paper is organised as follows. Section II describes the modulation strategy and soft-switching technique in details. Key simulation results are presented in section III to verify proposed operation of the converter.

II. Steady state operation

A detailed discussion on steady state operation of the converter is presented in this section. Considering UPF operation of the converter, the pulse width modulation strategy of the cyclo-converter is discussed in details. Generation of gating signals of all the switches and soft-switching techniques are also described in this section.

A. Generation of PWM AC: cyclo-converter

To describe the PWM strategy of the cyclo-converter an equivalent circuit configuration is shown in Fig.2. In this figure Q_X represents top switch pair i.e Q_{X1}, Q_{X2} and Q'_X represents bottom switch pair Q_{X3}, Q_{X4} of the cyclo-converter. Here, X denotes the three phases a, b and c. Q_X and Q'_X are complimentary switched. The

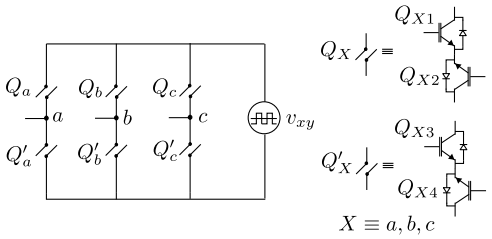

Fig. 2. Equivalent circuit representation of the AC side cyclo-converter

switching state of the converter is defined as follows: if the top switch Q_X (either Q_{X1} or Q_{X2}) is ON $\Rightarrow$ switching state is 1. If the bottom switch Q'_X (either Q_{X3} or Q_{X4}) is ON $\Rightarrow$ switching state is 0. According to the above definition, the cyclo-converter has six active switching states and two zero states. For example, switching state (110) indicates the switches Q_a,Q_b and Q'_c are ON. The input AC line currents (i_{ga}, i_{gb}, i_{gc}) are assumed to be ripple free and are in same phase with the average line to neutral pole voltages $(\overline{v}_{an_t}, \overline{v}_{bn_t}, \overline{v}_{cn_t})$ generated by the cyclo-converter. The three phase input currents and average pole voltages of the cyclo-converter are given as-

$$\begin{aligned} i_{ga} &= I_m \cos(\omega t) \\ i_{gb} &= I_m \cos\left(\omega t - \frac{2\pi}{3}\right) \\ i_{gc} &= I_m \cos\left(\omega t + \frac{2\pi}{3}\right) \end{aligned} \tag{1}$$

$$\begin{aligned} \overline{v}_{an_t} &= V_m \cos(\omega t) \\ \overline{v}_{bn_t} &= V_m \cos\left(\omega t - \frac{2\pi}{3}\right) \\ \overline{v}_{cn_t} &= V_m \cos\left(\omega t + \frac{2\pi}{3}\right) \end{aligned} \tag{2}$$

where $\omega = 2\pi f$ and f is the line frequency, V_m and I_m are the peak values of the average line to neutral voltage and input current respectively. The cyclo-converter output voltage space vector is defined as-

$$V_S = \left(\overline{v}_{an_t} + \overline{v}_{bn_t} e^{j\frac{2\pi}{3}} + \overline{v}_{cn_t} e^{-j\frac{2\pi}{3}}\right) = \frac{3}{2} V_m e^{j\omega t} \tag{3}$$

Based on the switching states of the cyclo-converter, there are six active voltage vectors $(V_1 - V_6)$ and two zero vectors (V_0, V_7) as shown in Fig. 3. Each active voltage vector corresponds to two distinct switching states of the cyclo-converter based on the polarity of the applied voltage, v_{xy}. For example, if $v_{xy} = +nV_{dc}$

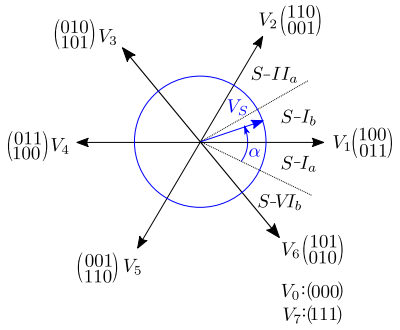

Fig. 3. Voltage space vectors of the cyclo-converter

where n is HFT turns ratio $\frac{N_1}{N_2}$ and V_{dc} is DC voltage, the switching state of the cyclo-converter (110) generates the space vector-

$$V_2 = n\left(V_{dc} + V_{dc} \cdot e^{j\frac{2\pi}{3}} + 0 \cdot e^{-j\frac{2\pi}{3}}\right) = nV_{dc} \cdot e^{j\frac{\pi}{3}} \tag{4}$$

Again when $v_{xy} = -nV_{dc}$, the switching state (001) gives the same voltage vector V_2. Altogether V_2 is represented as

$$V_2 \Rightarrow V_2 \begin{pmatrix} 110 \\ 001 \end{pmatrix} \tag{5}$$

The voltage vector space is divided into six equal sectors $(I - VI)$ and each sector is further divided into two equal sub-sectors e.g. sector I is divided into I_a and I_b. These sectors and their angular spreads are given in Table I.

The average voltage vector V_S is synthesized using following vector sequence: $(V_1 - V_2 - V_7) - (V_1 - V_2 - V_0)$ in sector I_b $(\omega t : (0, \frac{\pi}{6}))$ over a switching cycle T_s as shown in Fig. 4. Similar vector sequences are followed in other sectors to generate average voltage vector V_S. The voltage vectors V_1, V_2 and V_7 are applied

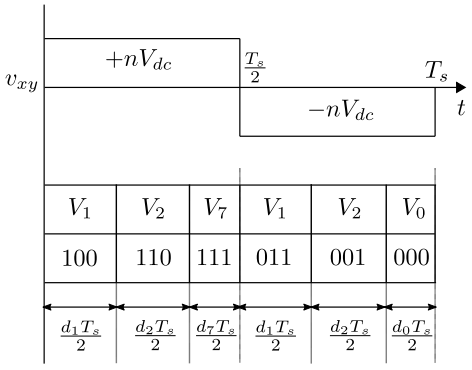

Fig. 4. Space vector sequence over a switching cycle in sector I_b

sequentially over $\frac{T_s}{2}$ for the following fractions of time: d_1, d_2 and d_7 respectively. These time intervals are estimated as follows. The average voltage vector-

$$\begin{aligned} V_S =& \frac{3}{2} V_m \cdot e^{j\omega t} \\ =& d_1 \cdot nV_{dc} + d_2 \cdot nV_{dc} e^{j(\frac{\pi}{3})} \end{aligned} \tag{6}$$

TABLE I. SECTORS IN THE VOLTAGE VECTOR SPACE

Sector	I	II	III	IV	V	VI
Angular Spread	$(-\frac{\pi}{6}, \frac{\pi}{6})$	$(\frac{\pi}{6}, \frac{\pi}{2})$	$(\frac{\pi}{2}, \frac{5\pi}{6})$	$(\frac{5\pi}{6}, \frac{7\pi}{6})$	$(\frac{7\pi}{6}, \frac{3\pi}{2})$	$(\frac{3\pi}{2}, \frac{11\pi}{6})$

By equating real and imaginary part of (6)

$$\begin{aligned} d_1 &= m \sin\left(\frac{\pi}{2} - \alpha\right) \\ d_2 &= m \sin\left(\alpha - \frac{\pi}{6}\right) \end{aligned} \tag{7}$$

The modulation index m and space vector angle α are given as-

$$\begin{aligned} m &= \frac{\sqrt{3} V_m}{n V_{dc}} \\ \alpha &= \left(\omega t + \frac{\pi}{6}\right) \end{aligned} \tag{8}$$

Again,

$$d_1 + d_2 + d_7 = 1 \tag{9}$$

as these intervals completely encompass $\frac{T_s}{2}$. From (7) and (9), d_7 is expressed as

$$d_7 = 1 - m \sin\left(\alpha + \frac{\pi}{6}\right) \tag{10}$$

As the voltage vectors applied are symmetrical over a switching cycle (see Fig. 4), HFT flux is balanced over a switching cycle. In this section v_{xy} is assumed to be square wave as shown in Fig. 4. In the next section generation of v_{xy} and the commutation process of the cyclo-converter is discussed in details.

B. Commutation process

The HFT has leakage inductance. Input currents i_{ga}, i_{gb} and i_{gc} are inductive in nature. Each time a switching transition happens in cyclo-converter, current through leakage inductor must be changed to avoid high voltage spike across the switches. This process is referred as commutation and is discussed in this section. What follows is a detailed description of commutation process in one half of the switching period (T_s) in sector I_b when $v_{AB} = V_{dc}$. v_{AB} is the applied voltage across the HFT terminals A, B (see Fig. 1). Similar commutation process is followed for next half of the switching period (when $v_{AB} = -V_{dc}$) with the symmetrical switches. Slowly varying properly filtered input line currents are considered as constant current sources (I_{ga}, I_{gb} and I_{gc}) in a switching period (T_s). In sector I_b $\left(0 < \omega t < \frac{\pi}{6}\right)$, input current polarities are given as- i_{ga} is positive and i_{gb}, i_{gc} are negative. Based on input current polarity, a phase current flows through either Q_{a2} and body diode of Q_{a1} or Q_{a3} and body diode of Q_{a4} depending on the applied switching state 1 or 0 of leg a respectively. Similarly in this sector following b and c leg switch-diode pairs of the cyclo-converter take part in conduction : for b phase current- either Q_{b4} and anti-parallel diode of Q_{b3} or Q_{b1} and diode of Q_{b2}, for c phase current- either Q_{c4} and anti-parallel diode of Q_{c3} or Q_{c1} and diode of Q_{c2}. The switching scheme of DC side H bridge and cyclo-converter switches is given in Table II. In this table for a switch or diode, 1 implies ON and conducting, 0 implies OFF and 1/NC means switch is ON but not conducting. D_{1-4} are the body diodes of switch S_{1-4} respectively.

a) Applied vector: $V_1(100)$ (Fig. 5a): In this switching state active switches $Q_{a2,b4,c4}$ and body diodes of $Q_{a1,b3,c3}$ of the cyclo-converter are conducting. In DC side, body diodes of S_1 and S_4 are conducting. The switching state applies a voltage $+V_{dc}$ across the transformer terminals A, B. The HFT voltage and current polarities shown in Fig. 5a indicate the active power flow from AC to DC side in this state. The HFT current i_p is given as

$$i_p(t) = I_{ga} = \mid I_{gb} \mid + \mid I_{gc} \mid \tag{11}$$

b) Transition: $V_1(100) \rightarrow V_2(110)$ (Fig. 5b): Switch Q_{b1} is turned ON. Due to transformer leakage inductance, current through Q_{b1} can not change immediately. So, this is a zero current (ZCS) turn ON event. The body diode of Q_{b2} is forward biased due to the transformer voltage polarity. Now the AC side transformer winding is shorted through b leg switches and diodes of the cyclo-converter. b phase current I_{gb} is transferred from Q_{b4} to Q_{b1} linearly with a slope $\frac{nV_{dc}}{L_{lk}}$, where L_{lk} is the equivalent leakage inductance seen from the cyclo-converter side of the HFT. The circuit equation in this interval is given as-

$$L_{lk} \frac{di_p(t)}{dt} + nV_{dc} = 0 \tag{12}$$

So the transformer current i_p starts falling from ($\mid I_{gb} \mid + \mid I_{gc} \mid$). At the end of this transition state i_p becomes $\mid I_{gc} \mid$. At this moment b phase current is completely transferred from Q_{b4} to Q_{b1}. The body diode of Q_{b3} is reverse biased.

c) Applied vector: $V_2(110)$ (Fig. 5c): In this state b phase current I_{gb} circulates through active switches Q_{a2}, Q_{b1} and body diodes of $Q_{a1,b2}$. As no current is flowing through Q_{b4}, it is now turned OFF ensuring ZCS. The HFT current $i_p(t) = \mid I_{gc} \mid$. In DC side, the body diodes D_1 and D_4 are conducting. Active power flows from AC to DC side.

d) Transition: $V_2(110) \rightarrow V_7(111)$ (Fig. 5d): Switches Q_{c1}, S_1 and S_4 are turned ON. The body diode of Q_{c2} is forward biased due to HFT voltage polarity. The transformer winding is again shorted through leg c cyclo-converter switches. The turned ON of Q_{c1} is L_{lk} assisted ZCS similar to Q_{b1} as described previously. Switching transitions of $S_{1,4}$ are zero voltage (ZVS) type as their body diodes are conducting. The c phase

TABLE II. SWITCHING STATES AND HFT VOLTAGE IN SECTOR I_b

	Q_{a2}	Q_{a3}	Q_{b1}	Q_{b4}	Q_{c1}	Q_{c4}	$S_{1,4}$	$D_{1,4}$	$S_{2,3}$	$D_{2,3}$	v_{AB}
V_1	1	0	0	1	0	1	0	1	0	0	V_{dc}
$V_1 \rightarrow V_2$	1	0	1	1	0	1	0	1	0	0	V_{dc}
V_2	1	0	1	0	0	1	0	1	0	0	V_{dc}
$V_2 \rightarrow V_7$	1	0	1	0	1	1	1/NC	1	0	0	V_{dc}
V_7	1	0	1	0	1	0	1/NC	0	0	0	V_{dc}
$V_7 \rightarrow V_1$	1	1	1	0	1	0	1	0	0	0	V_{dc}
V_1	0	1	1	0	1	0	0	0	0	1	$-V_{dc}$

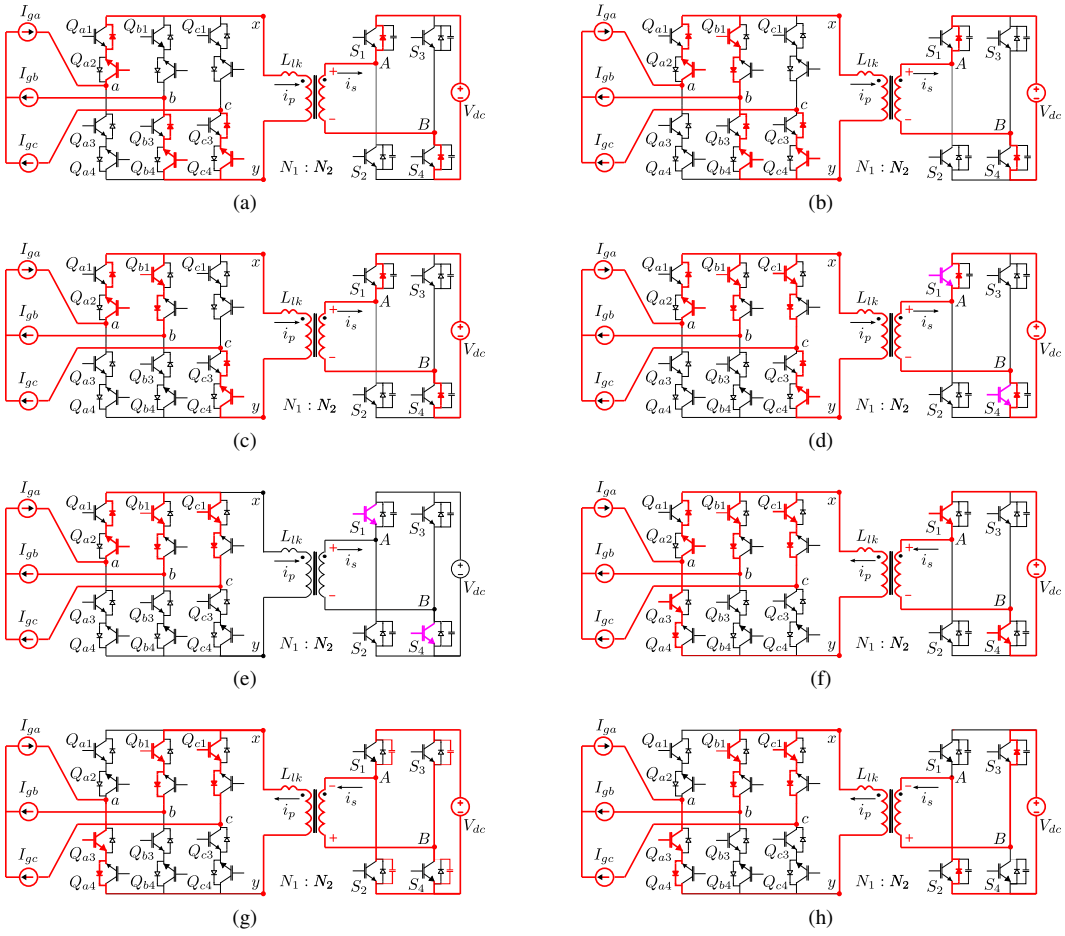

Fig. 5. Switching states and commutation process.

current I_{gc} is transferred from Q_{c4} to Q_{c1} linearly. The circuit equation is same as in (12). At the end of this transition, transformer current $i_p(t)$ falls to zero linearly with slope $\frac{nV_{dc}}{L_{lk}}$, I_{gc} is completely transferred from Q_{c4} to Q_{c1} and the body diode of Q_{c3} is reverse biased.

e) Applied vector: $V_7(111)$*(Fig. 5e):* In this switching state line currents are free-wheeling through active switches $Q_{a2,b1,c1}$ and the body diodes of $Q_{a1,b2,c2}$. The transformer current i_p is zero. As the switches S_1 and S_4 are ON, a positive voltage V_{dc} is still applied across the transformer terminal A, B. To ensure ZCS transition, Q_{c4} is turned OFF in this state. This is a zero state i.e no active power transfer in this interval.

f) Transition: $V_7(110) \rightarrow V_1(011)$ *(Fig. 5f):* Switch Q_{a3} is turned ON. This is again a leakage inductance assisted ZCS transition. As $S_{1,4}$ are ON and a positive voltage is applied across A,B, the body diode of Q_{a4} is forward biased. Now the transformer terminals x, y are shorted through $Q_{a2,a3}$ and body diodes of $Q_{a1,a4}$. The circuit equation is given by (12). The primary current $i_p(t)$ starts growing in opposite direction from zero. Thus the polarity of the transformer

current is reversed. a phase current I_{ga} is transferred linearly from Q_{a2} to Q_{a3}.

When I_{ga} is completely transferred to Q_{a3}, body diode of Q_{a1} is reverse biased. At this instant the transformer current i_p is given as

$$i_p = -I_{ga} = -(\mid I_{gb} \mid + \mid I_{gc} \mid) \tag{13}$$

After this moment, the switch Q_{a2}, S_1 and S_4 are turned OFF. Turn OFF of Q_{a2} is ZCS as no current is flowing through the switch. Due to presence of device parasitic capacitance across S_{1-4}, voltage can not change immediately. So, turn OFF of $S_{1,4}$ are zero voltage type transitions. Transformer current i_s starts charging the device capacitances of $S_{1,4}$ linearly and discharging the device capacitances of $S_{2,3}$ (see Fig. 5g). The circuit equations are given as-

$$\begin{aligned} i_p &= -I_{ga} \\ i_s &= -ni_p \\ i_s &= C\frac{dv_1}{dt} - C\frac{dv_2}{dt} \\ i_s &= C\frac{dv_4}{dt} - C\frac{dv_3}{dt} \\ v_1 &+ v_2 = v_3 + v_4 = V_{dc} \end{aligned} \tag{14}$$

where, v_{1-4} and C are the voltages and parasitic capacitances across the devices S_{1-4} respectively. Solving (14) v_2 and v_3 are given as-

$$v_2(t) = v_3(t) = V_{dc} - \frac{nI_{ga}}{2C}t \tag{15}$$

At the end, device capacitances of $S_{2,3}$ are fully discharged and the body diodes are forward biased and starts conducting.

g) Applied vector: $V_1(011)$ (Fig. 5g): In this state active switches $Q_{a3,b1,c1}$ and body diodes of $Q_{a4,b2,c2}$ of the cyclo-converter are conducting. In DC side as the body diodes of S_2 and S_3 are conducting a negative voltage $-V_{dc}$ is applied across the transformer terminals A,B. The HFT voltage and current polarity indicated in Fig. 5g shows the active power flow from AC to DC side in this interval.

The switching states in the next half switching period are identical to the states discussed in detail for the first half.

III. Simulation Results

The converter is simulated using described modulation strategy in MATLAB simulink. The input of the converter connected to 400 V, 50 Hz grid. Desired output voltage is 600V DC. The simulation parameters are given in Table III. The converter is switched at 10 kHz. Fig. 6a shows 3ϕ input voltage ($v_{ga,gb,gc}$) and current ($i_{ga,gb,gc}$) waveforms. The input current waveforms have a peak of approximately 250 A. The input currents lag the grid voltages due to line filter inductances. The input power factor is 0.97. Fig. 6a also presents filtered

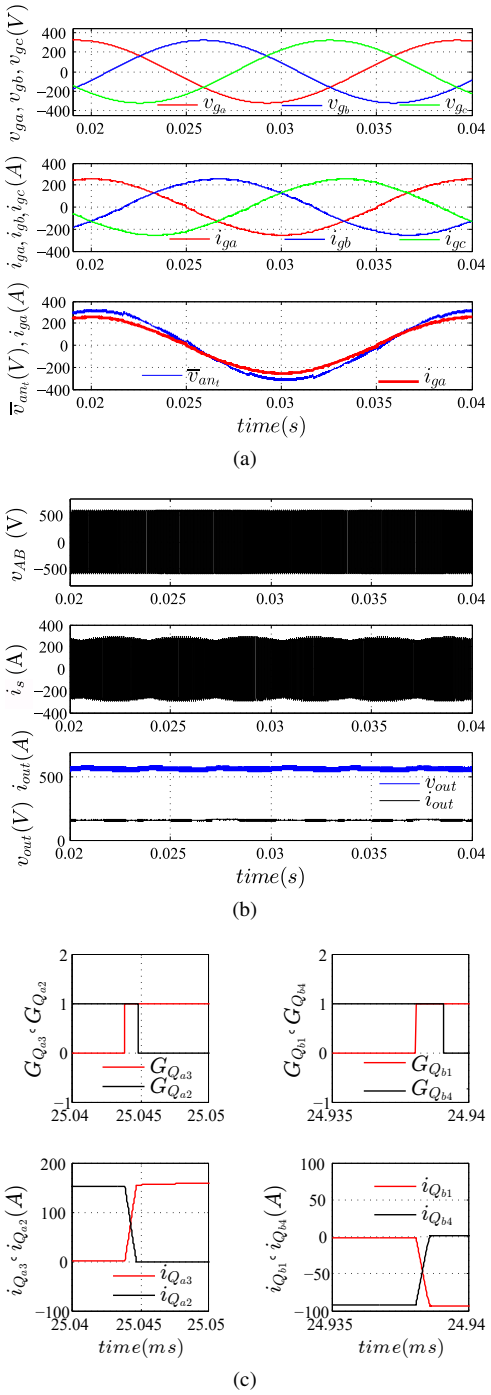

Fig. 6. Simulation waveforms- (a) Input voltage and current waveforms, (b) HFT secondary voltage and current; DC output voltage and current (c) Soft-switching (in $S-II$)

TABLE III. SIMULATION PARAMETERS

Parameter	Value
Input AC (V)(L-L RMS)	400
Output DC (V)	600
Power (kW)	118
Line frequency (f) (Hz)	50
Switching frequency	10kHz
HFT turns ratio	100:100
Modulation index (m)	0.91
Filter inductance	$0.980mH$
HFT leakage impedance	$2.0\mu H$
Device capacitance	10 nF

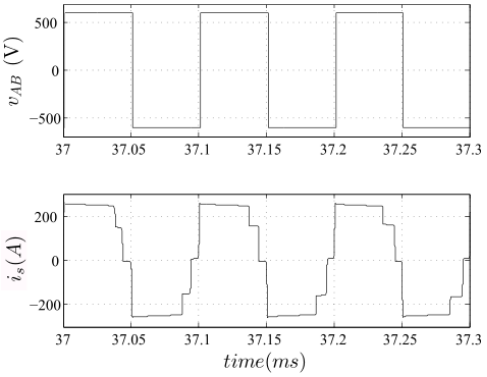

(a)

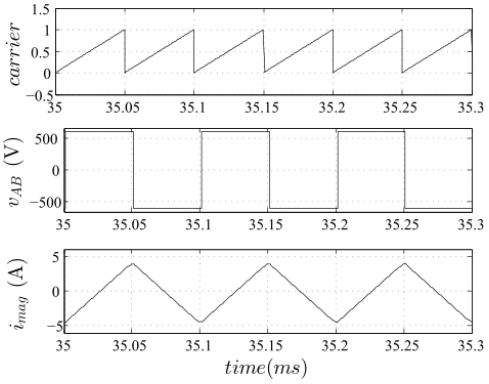

(b)

Fig. 7. Simulation waveforms- (a) HFT voltage and current waveform, (b) Flux balance in high frequency switching cycle

average pole voltage $\overline{v}_{an_t}$ of the cyclo-converter with the line current i_{ga}. $\overline{v}_{an_t}$ has a peak of approximately 316 V and is almost in phase with i_{ga}. The HFT voltage and current waveforms over a line cycle are shown in Fig. 6b. The output DC voltage and current waveforms are also shown in Fig. 6b. The average DC output current is approximately 197 A. Fig.6c shows the commutation process of the switches $Q_{a2,a3}$ and $Q_{b1,b4}$ in sector I_b. Switching strategy ensures ZCS of these switches. Initially Q_{a2} was conducting. After Q_{a3} is turned ON current transfers linearly from Q_{a2} to Q_{a3}. The gating pulse of Q_{a2} is removed only after the current becomes zero. Fig. 7a shows the HFT secondary voltage and current in a switching cycle. This wave form shows the changes in the transformer current during commutation in a switching cycle. Fig. 7b shows the magnetizing current waveform of the transformer with the applied terminal voltage. Area under the positive half cycle of the magnetising current is approximately equal to area under the negative half cycle. Thus this figure verifies the flux balance in the transformer core over a switching cycle.

IV. CONCLUSION

In this paper a novel modulation strategy for active rectification of a three phase single stage isolated DC-AC converter has been proposed. The proposed modulation strategy has following advantages- i) the AC side switches are zero current (ZCS) switched , ii) DC side switches are zero voltage switched, iii) no additional snubber for soft-switching, iv) loss less switching at all load condition, v) transformer flux balance over a switching cycle. The steady state converter operation is discussed in details. The simulation results verify the converter operation. In conclusion the proposed strategy results in high power density and highly efficient isolated three phase rectifier with near unity power factor operation. This can be promising solution for the applications like- battery chargers for electric vehicle, UPS systems and front end converter of server power supplies.

REFERENCES

[1] T. Kawabata, *et.al*, "High frequency link dc/ac converter with pwm cycloconverter," in Industry Applications Society Annual Meeting, 1990., Conference Record of the 1990 IEEE, pp. 1119-1124, IEEE, 1990.

[2] M. Matsui, *et.al*, "High frequency link dc/ac converter with suppressed voltage clamp circuits-naturally commutated phase angle control with self turn off devices," IEEE Transactions on Industry Applications, vol. 32, no. 2, pp. 293-300, 1996.

[3] M. A. Rodrigues, *et.al* , "Pwm strategy for switching loss reduction in a high frequency link dc to ac converter," in Power Electronics Specialists Conference, 1999. PESC 99. 30th Annual IEEE, vol. 2, pp. 789-794, IEEE, 1999.

[4] B. Ozpineci and B. Bose, "Soft-switched performance-enhanced high frequency non resonant link phase-controlled converter for ac motor drive," in Industrial Electronics Society, 1998. IECON98. Proceedings of the 24th Annual Conference of the IEEE, vol. 2, pp. 733-739.

[5] S. Norrga, S. Meier, and S. Ostlund, "A three-phase soft-switched isolated ac/dc converter without auxiliary circuit," IEEE transactions on industry applications, vol. 44, no. 3, pp. 836 - 844, 2008.

[6] X. Yu and M. Wang, "An isolated bi-directional soft-switched three phase dc-ac matrix-based converter with novel unipolar spwm and synchronous rectification," in Transportation Electrification Conference and Expo (ITEC), 2016 IEEE, pp. 1-7, IEEE, 2016.